

### 3. Measurement methods

This chapter briefly introduces the available bioimpedance measurement methods based on contact electrodes: the two-electrode method, the three-electrode method and the four-electrode method.

The four-electrode method is the best choice for soft tissues but it is not error free. It can be found that the error sources limit the useful bandwidth of the measurement probe. In the case of the MicroCard probe such a useful band goes from 100 Hz to 100 kHz.

Here it is also justified the injected current level for the measurement. It is not only limited for safety reasons but also to avoid nonlinear phenomena of living tissues.

A novel measurement method based on five electrodes is presented and analyzed. It is intended to minimize errors at low frequencies caused by the high electrode-electrolyte interface impedances. Unfortunately, although this five-electrode method works, some limitations have been found that made almost impossible its implementation for living tissue measurements.

### 3.1. Two-electrode method

The most evident way to perform electrical impedance measurements by using electrodes is to apply the two-electrode method, also referred as the bipolar method. That is, to inject a known current into the device under test (DUT)<sup>1</sup> through two electrical contacts and to measure the resulting voltage drop between these two contacts (see Figure 3.1).

This method only works properly if the impedance of the electrical contacts ( $Z_{C+}$  and  $Z_{C-}$ ) is much lower than the impedance of the DUT ( $Z_{DUT}$ ) since the measured impedance ( $Z'$ ) is the sum of  $Z_{DUT}$ ,  $Z_{C+}$  and  $Z_{C-}$ . As it has been seen in the previous chapter, the electrode-electrolyte interface impedances can be higher than the impedance under test, especially at low frequencies, and are too instable and unpredictable to think of a mathematical correction of the measurement. Therefore, the repeatability and the reproducibility of the measurements will be seriously compromised.

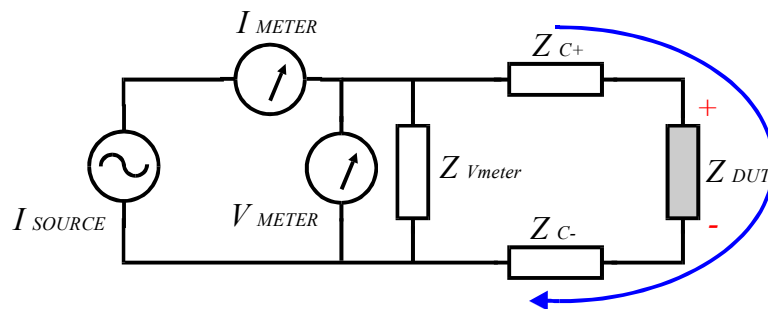


**Figure 3.1.** Schematic representation of the two-electrode method.

The input impedance of the meter and the parasitic capacitances also degrade the performance of the measurement system, particularly at high frequencies. However, in some cases, if the behavior of these parasitic elements can be modeled with a resistance or a capacitance and some *a priori* information exists about the material under test (e.g. that it is pure resistive), then, it is possible to mathematically compensate the measurement. That is an interesting option since at high frequencies the electrode-electrolyte interface impedances will be low and will not distort the measurement.

Although the use of the two-electrode method can be justified in some applications such as skin [1;2] or dental [3] studies in which the sample impedance is much higher than the electrode impedance at the working frequencies, its use in soft tissues is nowadays very rare [4] and questionable.

<sup>1</sup> This term has been borrowed from electronics. Probably it would be more convenient to use Sample Under Test (SUT).

### 3.2. Four-electrode method <sup>2</sup>

The four-electrode method, also referred as tetrapolar or Kelvin method, has been used to measure the resistivity of materials since the late 1800's [5]. It uses a pair of electrodes to inject the current into the sample and another pair of electrodes to measure the resulting voltage drop (Figure 3.2). In principle, because no current flows through the voltage meter ( $Z_{V\text{meter}} \rightarrow \infty$ ), the injected current completely flows through the sample and the voltage drop at the sample is the same that the meter 'sees'. Thus, in principle, the electrode-electrolyte interface impedance has no influence on the measurement.

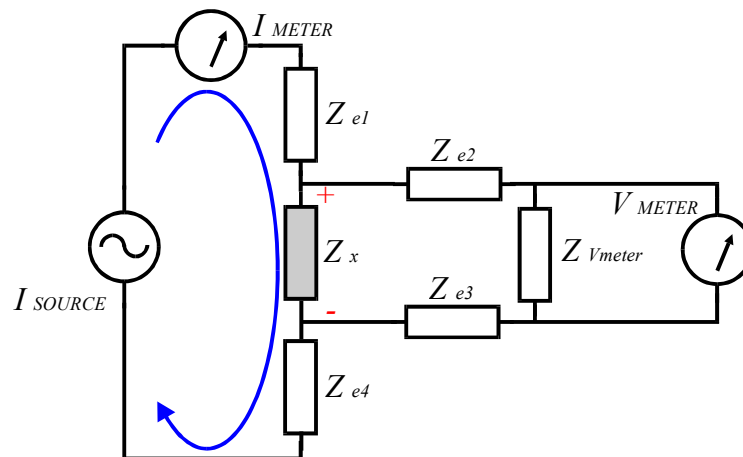


**Figure 3.2.** Schematic representation of the four-electrode measurement method.

However, the true fact is that the electrode-electrolyte interface impedance has influence on the measurements, particularly at low frequencies where its magnitude can be very large. The reason for this is that the electrode impedances cause common voltages that cannot be completely rejected by the differential amplifier of the voltage meter. For instance, consider that the ground of the electronic circuitry in Figure 3.2 is connected to the current collecting electrode (e4), then, the impedance of this electrode causes a voltage drop ( $\sim I \cdot Z_{e4}$ ) that appears as a common voltage to be rejected at the inputs of the voltage meter. Unfortunately, the situation is even worse than that since the inner electrode impedances and the input parasitic impedances of the voltage meter cause a decrease of the effective Common Mode Rejection Ratio (CMRR). Part of the common voltage at the sample is transformed into differential voltage at the differential amplifier inputs (Figure 3.3). This phenomenon has been analyzed by

<sup>2</sup> When applying the four-electrode method it would be more precise to talk of *trans-impedance* than to use the term *impedance* since a two-port system is involved and a transfer parameter is computed (current is injected in one port and voltage is recorded in the other port). However, for the sake of simplicity here it will be used the word *impedance* as most authors do.

Pallás-Areny and Webster [6] and it can be concluded that it is desirable to make input impedances as large and balanced as possible.

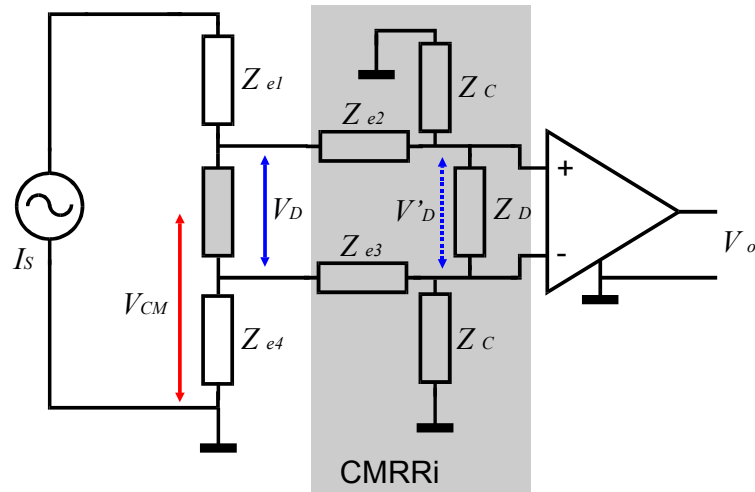


**Figure 3.3.** The effective CMRR is reduced because of the electrode interface impedances and the common and differential input impedances of the differential amplifier.

At high frequencies, the influence of parasitic capacitances is manifested (Figure 3.4). Several errors are caused by those parasitic impedances: the current flowing through the sample is reduced (shunting caused by  $Z_{14}$ ), the differential gain is reduced (shunting caused by  $Z_{24}$ ), part of the current is directly injected at the differential amplifier input (through  $Z_{12}$  and  $Z_{13}$ )... Those parasitic capacitances<sup>3</sup> mainly consist of stray capacitances between the electrode leads and the input capacitances of the instrumentation.

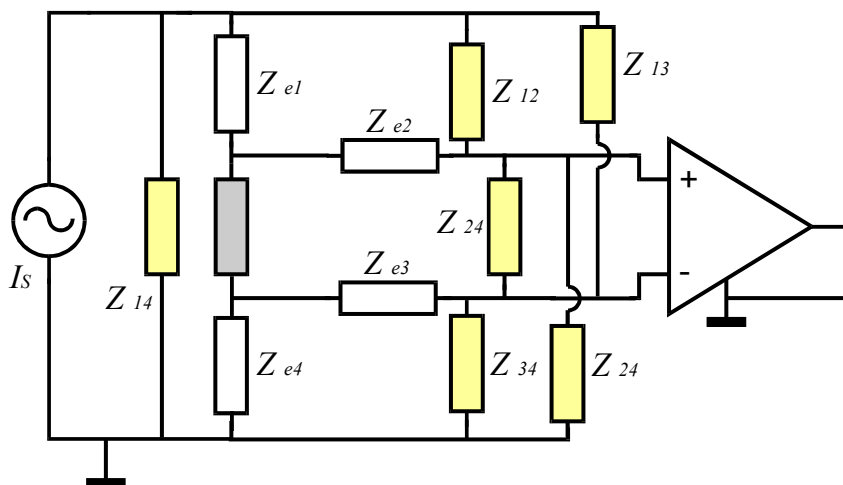


**Figure 3.4.** Possible parasitic impedances.

<sup>3</sup> Annex C provides some advices and methods to reduce their influence.

All these error sources can be analytically studied but the resulting expressions are too cumbersome for practical purposes. It is more convenient to make use of computer simulations. By using electrical circuit simulators, such as SPICE, it is possible to introduce all these elements and to obtain results close to the actual measurements or, what is more interesting, to estimate the error margins in the case of living tissue measurements.

The results shown in Figure 3.5 correspond to the simulation of the silicon bioimpedance probe when measuring a saline solution (NaCl 0.9%). The parameters used for the simulation are similar to the actual ones and, as it can be observed, the results from the simulation are also quite similar to the actual measurements (see Annex D). Some degree of unbalance (30%) between the inner electrodes has been introduced in order to manifest the error at lower frequencies, otherwise no error would be obtained at those frequencies.

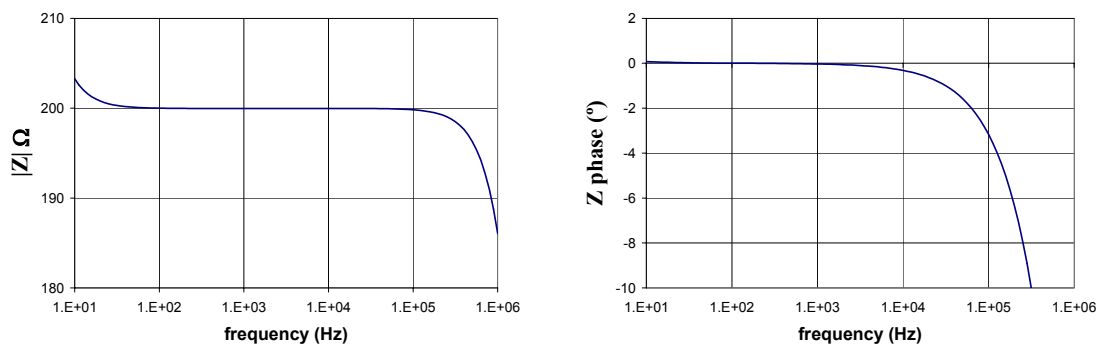


**Figure 3.5.** Simulated four-electrode measurement (impedance magnitude and phase) in the case of a MicroCard probe immersed in saline solution. ( $Z_x = 200 \Omega$ ;  $Z_{e1} = Z_{e3} = Z_{e4} = 1500 \Omega + 800 \text{ nF}$ ;  $Z_{e2} = 1000 \Omega + 600 \text{ nF}$ ;  $Z_{12} = Z_{13} = Z_{14} = Z_{23} = Z_{24} = Z_{34} = 10 \text{ pF}$ ;  $Z_{in+} = 8 \text{ pF} // 50 \text{ M}\Omega$ ;  $Z_{in-} = 8 \text{ pF} // 50 \text{ M}\Omega$ ).

The simulation results shown in Figure 3.6 would correspond to the measurement of an hypothetic living tissue (purely resistive tissue,  $\rho = 700 \Omega \cdot \text{cm}$ ). The errors at high frequencies are larger than in the previous case since the sample impedance is higher and, therefore, more current tends to flow through the parasitic capacitances. Nevertheless, it is even more significant the distortion at low frequencies. The cause of this is that the simulated electrode interface impedances are much larger and much more unbalanced than in the saline solution case<sup>4</sup>. This imitates what happens in actual measurements due to the heterogeneity of the living tissues. Therefore, it must be taken into account that the low frequency errors in the case of living tissue measurements are much larger than those obtained when measuring saline solutions.

<sup>4</sup> Those simulated electrode impedance values are in agreement with the experimental results described in chapter 2.

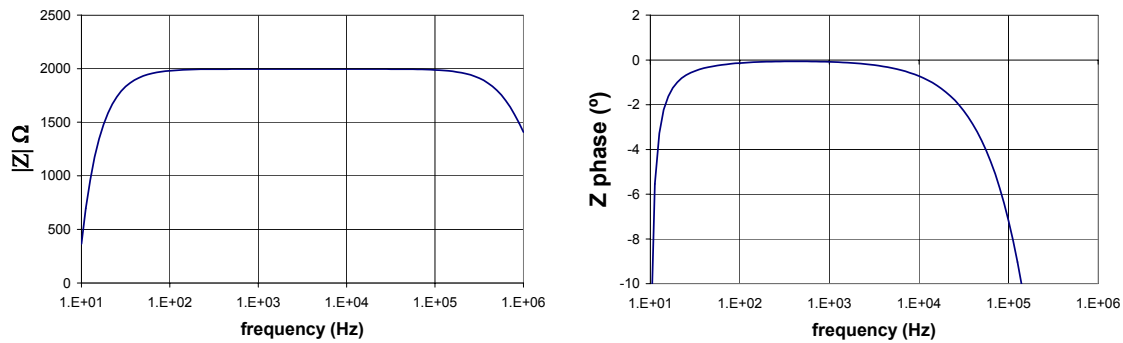


**Figure 3.6.** Simulated four-electrode measurement (impedance magnitude and phase) in the case of a MicroCard probe inserted into a tissue. ( $Z_x = 2000 \Omega$ ;  $Z_{e1} = Z_{e3} = Z_{e4} = 1000 \Omega + 80 \text{ nF}$ ;  $Z_{e2} = 1500 \Omega + 30 \text{ nF}$ ;  $Z_{12} = Z_{13} = Z_{14} = Z_{23} = Z_{24} = Z_{34} = 10 \text{ pF}$ ;  $Z_{in+} = 8 \text{ pF} // 50 \text{ M}\Omega$ ;  $Z_{in-} = 8 \text{ pF} // 50 \text{ M}\Omega$ ).

It must be noted that in the above simulations the electrode-electrolyte interface impedance has been modeled as capacitance. That oversimplification lessens the actual distortion at low frequencies. Since a CPE decays more slowly in the frequency domain than a capacitance, the influence of the electrode-electrolyte interface impedance is extended over a broader frequency range than what is obtained in the simulations. Nevertheless, for the sake of simplicity<sup>5</sup>, it is reasonable to employ capacitances to model the interface impedance.

### 3.3. Three-electrode method

As it has been shown by some authors [8;9], if the area of electrode 4 (Figure 3.2) is made sufficiently large (e.g. by using a large metal plate or foil), its interface impedance can be reduced in order to make unnecessary the electrode 3 (the voltage meter is connected to electrode 2 and electrode 4) and to simplify the measurement set-up.

This must not be confused with the three-electrode potentiostat used in electrochemistry [10]. In that case the objective is to study the electrical properties of an electrode-electrolyte interface.

<sup>5</sup> In some SPICE software, such as Hspice (Sun/Unix platforms), it is possible to introduce elements whose impedance depends on frequency. In such cases it is straightforward to model the CPE. Otherwise, smarter solutions are required. For instance, it is possible to roughly model the CPE with a set of distributed resistance and capacitance pairs [7].

### 3.4. Injected current intensity for bioimpedance measurements

It is clear that large currents are interesting to enlarge the voltage drop and, consequently, to maximize the signal-to-noise ratio. However, two facts limit the allowable current intensity:

- Nonlinear behavior of the living tissues. As most physical phenomena, electrical bioimpedance reaches the nonlinear regime if the stimuli surpasses a certain value.
- Safety. The injected electrical energy can cause different sorts of damage to the living tissues.

In living tissues, the voltage/current relation is linear while the applied electrical fields do not reach the nonlinear threshold [11]. The closing or opening of ionic channels [12] on the cell membrane are usually pointed out as the responsible of such a nonlinear behavior: in the rest state, the cell membranes are polarized at about 10 kV/mm (voltage differences between the intra and extracellular media around tens of mV), if an electric field is superimposed, the protein structures on the cellular membrane that are responsible for the transport of specific ions can change their conformation and alter the conductivity of the membrane or, in a more extreme case, induce an ionic redistribution that reverses the membrane polarization (i.e. action potential).

Since local electric field is proportional to current density ( $E=J\rho$ ), the nonlinear threshold for a given tissue is usually expressed as a current density threshold. A rare and extreme case is that of human skin which can shown nonlinear behavior at current densities as low as  $100 \mu\text{A}/\text{cm}^2$  at 100 Hz <sup>6</sup>.

The nonlinear impedance response of living tissues must not be confused with the nonlinear impedance response of the electrode-tissue interface, or electrode-electrolyte interface. This phenomenon has been studied experimentally [14;15] and theoretically [16]. Its influence in the case of four-electrode measurements is not significant if the demodulation is able to reject the generated harmonics.

Living tissues can be damaged by electrical energy through three mechanisms [17]: thermal injury, electroporation and fibrillation. In the framework of this thesis work, the myocardium fibrillation is the only issue that must be addressed. Thermal injury and electroporation become irrelevant since their respective current and voltage thresholds are much larger.

No previous work has been found that clearly justifies the current amplitude for the electrical bioimpedance measurement of the heart by using the four-electrode method. In general, it seems that the criterion to select the current amplitude has been to use a

---

<sup>6</sup> Probably this is caused because the current flow is constrained through special zones of high conductance [13].

current below  $10 \mu\text{A}_{\text{RMS}}$  since this is the maximum allowable leakage current by the safety standards in the low-frequency range [18]. However, studies with larger currents have also been carried out [19] because low frequencies were not applied.

Therefore, the objective of this section is to determine and justify a current threshold for the heart case. The fibrillation threshold is determined for safety reasons and the cardiac excitation threshold (i.e. stimulation) is considered to be close to the nonlinear threshold.

The following discussion is completely based on the data extracted from [20]. That book chapter is basically a review of experimental studies in animals and humans relating to the effects of electrical current on cardiac tissues (stimulation, fibrillation, burns...). The original purpose of those experimental data was the therapeutic use of cardiac stimulation for cardiac pacing or defibrillation. However, that knowledge can also be applied to electrical safety concerns assuming some limitations.

The sensitivity of the heart to externally applied electrical currents depends critically on the timing of the stimulus with respect to the cardiac cycle. Thus, it is quite reasonable to think that the stimulation of a limited group of myocytes (cardiac cells) also depends on this timing. However, since the bioimpedance application will not be aware of this cycle (current pulses are randomly injected or permanent AC current is injected with a random start time), the worst case for excitation (just after the T ECG interval) must be considered.

#### Ventricular fibrillation (VF)

When an AC current of limited duration is injected, there exists a dependence of the current density VF threshold on electrode size. In the case of MicroCard electrodes (area  $\sim 900 \times 10^{-6} \text{ cm}^2$ ) this threshold would be approximately  $400 \text{ A/m}^2$  at 60 Hz. However, if this value is reduced in accordance with the electrode location sensitivity, the VF threshold would be  $180 \text{ A/m}^2$ . Thus, the maximum allowed current to avoid VF using MicroCard probes at frequencies<sup>7</sup> below 100Hz would be  $16 \mu\text{A}_{\text{RMS}}$ . If it is assumed that the thresholds given by the previous studies represent the 50% possibility of VF then, the limit should be scaled down by a 2.5 factor to make insignificant the possibility of VF. In this case, the safe value to avoid VF is  $6.4 \mu\text{A}_{\text{RMS}}$  which is below the  $10 \mu\text{A}_{\text{RMS}}$  threshold from safety standards. This somewhat surprising result is caused by the singular dimensions of the MicroCard electrodes.

#### Cardiac excitation (Ex)

Since the electric cardiac excitation is a manifestation of a nonlinear behavior of the cell membrane (initiation of action potentials) due to the electric local field, it is reasonable to think that the Ex current density threshold is constant for different electrodes sizes. The experimental data agree with this hypothesis for a wide range of electrode areas

---

<sup>7</sup> The frequency band from 10Hz to 100 Hz is the most dangerous band for VF.



(e.g. from 0.1 to 1 cm<sup>2</sup> the current density threshold is about 3 mA/cm<sup>2</sup>) but in the case of very small electrodes (<0.005 cm<sup>2</sup>) the current density threshold is significant higher (14 mA/cm<sup>2</sup> for 2 ms DC pulses). Thus, if the threshold current density is extrapolated to the MicroCard case at 50 Hz, the current threshold for stimulation is 12  $\mu$ A<sub>RMS</sub> which is larger than the VF limit (it must be taken into account that a very high safety factor has been introduced to calculate the VF current limit).

Taking the above into consideration, a 5  $\mu$ A<sub>RMS</sub> threshold has been chosen for myocardium impedance measurements by using the MicroCard probe at 1 kHz.

### 3.5. Five electrode method <sup>8</sup>

As it has been pointed out, high common voltage and limited CMRR can compromise the performance of the four-electrode method, particularly at low frequencies. It is always advisable to reduce the electrodes impedance (common voltage reduction) and to increase and to match the input impedances at the differential amplifier inputs as much as possible (effective CMRR enhancement). Apart from that, there are some circuitry strategies that can be applied to reduce the common voltage. These strategies are based on feeding back the common voltage measured at the differential amplifier to the current source (by driving its floating ground) or to the sample (by driving the current collecting electrode or by driving a fifth electrode connected to the sample) [21;22]. However, the requirement of floating parts or the precautions that must be taken into account to avoid instability could limit their application in some cases.

Here it is presented a new method that minimizes the error caused by the common voltage and that overcomes some of the drawbacks of the previous strategies by using a five-electrode probe. Briefly, two four-electrode impedance measurements are performed sequentially using two different electrodes to inject the current and a corrected impedance value is computed. Up to a point, this method could be understood as an *in situ* or in line calibration procedure

Figure 3.7 shows the arrangement of the electrodes and the switch that is needed to use the proposed method. At time  $t_1$  the switch selects electrode 1 as the injection electrode. This implies that the current applied by the four-electrode Impedance Analysis System (IAS) flows through the sample from electrode 1 to electrode 4.  $Z_{m1}$  is the result obtained from this measure and  $Z_{m2}$  is the measure obtained when the switch selects electrode 5 and the currents flows from this electrode to electrode 4.

If the electrical properties of the sample are homogenous and isotropic, there is a constant scalar relation between the applied current (I), the complex conductivity ( $\sigma^*$ )

---

<sup>8</sup> The contents of this section were partially presented in:

Ivorra, A. and Aguiló, J. New five-electrode method for impedance measurement. 263-266. 17-6-2001. Oslo, Norway. XI International Conference on Electrical Bio-Impedance (ICEBI). 17-6-2001.

and the resulting voltage drop between the measuring points (V). The constant that relates all these parameters is called cell factor (k) and only depends on the geometry of the impedance probe:

$$\frac{1}{Z} \stackrel{\Delta}{=} \frac{I}{V} = k \cdot \sigma \quad (3.1)$$

The value of k can be obtained mathematically for some electrode configurations<sup>9</sup> but, in most cases, it will be preferable to obtain it by measuring the impedance value (Z) in a medium with known conductivity.

In the present case, there are two different cells and, therefore, two cell constants can be defined:  $k_1$  for the cell constituted by the electrodes 1,2,3 and 4 and  $k_2$  for the cell constituted by electrodes 5,2,3 and 4. The relation between these two values is:

$$\lambda \stackrel{\Delta}{=} \frac{k_2}{k_1} = \frac{Z_1}{Z_2} \quad (3.2)$$

where  $Z_1$  and  $Z_2$  are the voltage-current ratios for each cell. This relation only depends on the probe geometrical configuration. Therefore, it is possible to obtain it under minim error conditions, for example, in a saline solution at a high enough frequency.

When a four-electrode measurement is being performed and the common voltage caused by  $Z_{E4}$  is considered as the unique error source, the measured impedance value ( $Z_m$ ) is:

$$Z_m = \frac{V + \frac{I \cdot Z_{E4}}{\text{CMRR}_e}}{I} = \frac{V}{I} + \frac{Z_{E4}}{\text{CMRR}_T} = Z + \frac{Z_{E4}}{\text{CMRR}_T} \quad (3.3)$$

where  $\text{CMRR}_T$  is the effective common mode rejection ratio as defined by Pallás-Areny and Webster [6]. Then, if two cells that share a common current collecting electrode ( $Z_{E4}$ ) are used to measure the same sample (same conductivity) it follows:

$$\frac{Z_1}{Z_2} = \lambda = \frac{Z_{m1} - \frac{Z_{E4}}{\text{CMRR}_T}}{Z_{m2} - \frac{Z_{E4}}{\text{CMRR}_T}} \Rightarrow \text{CMRR}_T^{-1} = \frac{Z_{m1} - \lambda \cdot Z_{m2}}{Z_{E4} \cdot (1 - \lambda)} \quad (3.4)$$

$$Z_1 = Z_{m1} - \frac{Z_{E4}}{\text{CMRR}_T} = Z_{m1} - \frac{Z_{m1} - \lambda \cdot Z_{m2}}{Z_{E4} \cdot (1 - \lambda)} \cdot Z_{E4} \Rightarrow Z_1 = \frac{\lambda}{\lambda - 1} \cdot (Z_{m1} - Z_{m2}) \quad (3.5)$$

<sup>9</sup> See chapter 2 and annex B.

Thus, in principle it is possible to compensate the influence of the common voltage caused by  $Z_{E4}$ . The requirement is to guarantee that in both impedance measurements the  $CMRR_T$  and  $Z_{E4}$  keep their values constant.

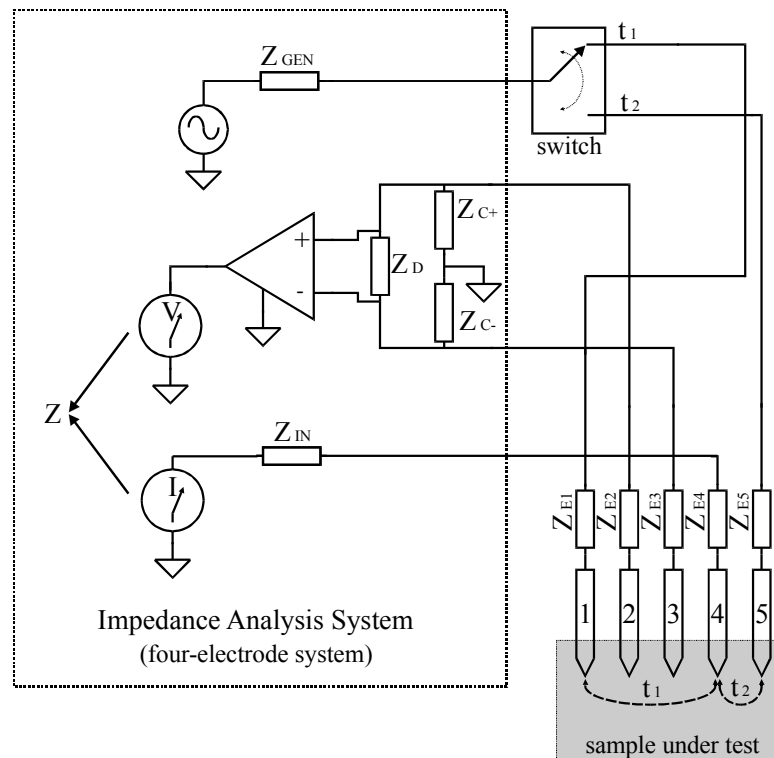


**Figure 3.7.** Schematic representation of the elements and the configuration that are needed to use the five-electrode method.

In order to demonstrate the feasibility of the proposed method, a prof-of-concept test was carried out. The configuration is the same that it is shown in Figure 3.7. The IAS is a Sorlartron 1260 Impedance Analyzer which is controlled through GPIB by a LabVIEW 5.1 program. This software also drives the relay that switches the injected current through electrode 1 or through electrode 5. For each analyzed frequency, two impedance measurements are sequentially performed and a compensated value is computed.

The five-electrode impedance probe was made using 0.5 mm length stainless steel needles ( $\varnothing$  0.7 mm) separated 2.5 mm on a plastic substrate. When this probe is immersed in NaCl 0.9% (9g/1000ml) solution the inter-electrode impedance is about  $15k\Omega \angle -70^\circ$  at 10Hz and  $77\Omega \angle -32^\circ$  at 10kHz. The  $\lambda$  value at 1 kHz is 5.05.

The results shown in Figure 3.8 correspond to a test performed in NaCl 0.9% solution which has a resistivity about  $70 \Omega \cdot \text{cm}$  and do not has any appreciable reactive behavior up to some tens of MHz. As it can be observed, the five-electrode method significantly improves the performance of the IAS, particularly for the impedance phase values. However, it does not totally cancel the errors at very low frequencies.

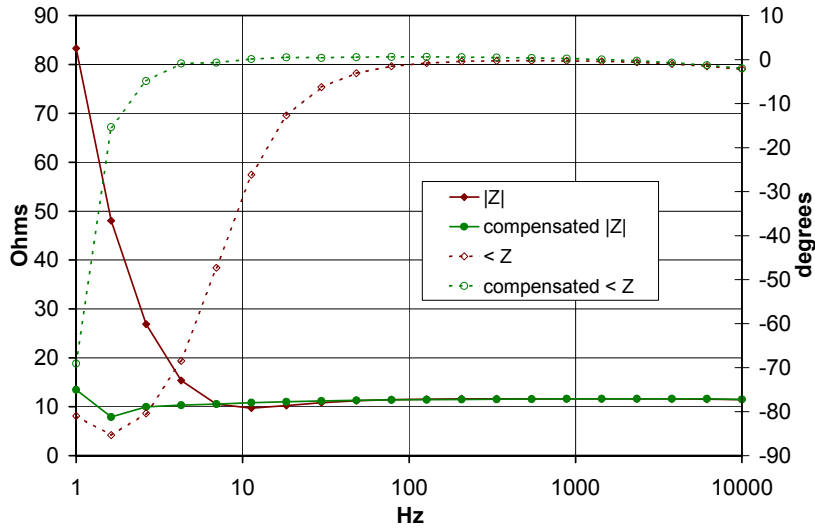


**Figure 3.8.** Impedance magnitude ( $|Z|$ ) and phase ( $\angle Z$ ) measured with Solartron 1260 and the compensated values obtained using the five-electrode method

After verifying that the inability of method to compensate the errors at very low frequencies was not caused by saturation, resolution or accuracy issues related with the IAS, it was determined that the method requisites (i.e.  $CMRR_T$  and  $Z_{E4}$  keep their values constant) were not met.

There is no reason to think that the effective  $CMRR$  is significantly modified between both measurements if they are performed quickly. On the other hand, it is known that the electrode impedance depends on many factors and one them is the injected current. That is, since the electrode impedance can be nonlinear [14;15] it seems reasonable to think that the current density differences between both measurements can cause  $Z_{E4}$  differences <sup>10</sup>.

In the case that  $Z_{E4}$  is not the same at both measurements ( $Z_{E4\_1}$ ,  $Z_{E4\_2}$ ):

$$\frac{Z_1}{Z_2} = \lambda = \frac{Z_{m1} - \frac{Z_{E4\_1}}{CMRR_T}}{Z_{m2} - \frac{Z_{E4\_2}}{CMRR_T}} \quad (3.6)$$

$$CMRR_T^{-1} = \frac{\lambda \cdot Z_{m2} - Z_{m1}}{\lambda \cdot Z_{E4\_2} - Z_{E4\_1}} \quad (3.7)$$

<sup>10</sup> I must thank Prof. Javier Rosell (UPC) for having pointed out this hypothesis.

$$Z_1 = \lambda \cdot \frac{Z_{m1} \cdot Z_{E4\_2} - Z_{m2} \cdot Z_{E4\_1}}{\lambda \cdot Z_{E4\_2} - Z_{E4\_1}} \quad (3.8)$$

which is equivalent to equation 3.5 in the case that  $Z_{E4\_1} = Z_{E4\_2} = Z_{E4}$ .

The additive error ( $\varepsilon$ ) of the five-electrode method caused by those differences can be analyzed by assuming that both E4 impedance values are related by a scalar<sup>11</sup>:

$$Z_{E4\_2} = \beta \cdot Z_{E4\_1} \quad (3.9)$$

$$Z_1 = \lambda \cdot \frac{Z_{m1} \cdot \beta \cdot Z_{E4\_1} - Z_{m2} \cdot Z_{E4\_1}}{\lambda \cdot \beta \cdot Z_{E4\_1} - Z_{E4\_1}} = \lambda \frac{Z_{m1} \cdot \beta - Z_{m2}}{\lambda\beta - 1} \quad (3.10)$$

$$Z_1 = Z_{C1} + \varepsilon = \frac{\lambda}{\lambda - 1} \cdot (Z_{m1} - Z_{m2}) + \varepsilon \quad (3.11)$$

$$\varepsilon = \lambda \left( \frac{Z_{m1} \cdot \beta - Z_{m2}}{\lambda\beta - 1} - \frac{Z_{m1} - Z_{m2}}{\lambda - 1} \right) \quad (3.12)$$

$$\varepsilon = \frac{\lambda \cdot (\beta - 1) \cdot (\lambda \cdot Z_{m2} - Z_{m1})}{(\lambda - 1) \cdot (\lambda\beta - 1)} \quad (3.13)$$

if it is assumed that the error of the four-electrode method is

$$\varepsilon_{\text{four-electrode}} \approx \frac{Z_{E4}}{\text{CMRR}_T} \quad (3.14)$$

then the error of the five electrode method is:

$$\varepsilon = \frac{\lambda}{\lambda - 1} (\beta - 1) \cdot \varepsilon_{\text{four-electrode}} \quad (3.15)$$

That indicates that impedance of electrode 4 must be constant ( $\beta \sim 1$ ) and  $\lambda$  must be as large as possible. Otherwise, larger errors than in the simple four-electrode measurement will be obtained. Unfortunately, those are almost opposite requirements; large  $\lambda$  values imply large current distribution differences and that leads to larger  $\beta$  values.

---

<sup>11</sup> The analysis can be also performed assuming that both values are related by a complex number, that would be the actual case. However, for the sake of simplicity, it is assumed that only the impedance magnitude is modified, not the phase.

The following experiment and its results support the hypothesis that the electrode impedance change is the major cause of the inability of the five-electrode method to compensate the errors at low frequencies:

A silicon probe with five electrodes (Figure 3.9) was employed to perform the measurement of a saline solution (NaCl 0.9%) by using the five-electrode method as in the previous experiment. The first electrode of current injection was  $I_{+1}$  and the second one was  $I_{+2}$ . This configuration leads to  $\lambda \sim 1.5$

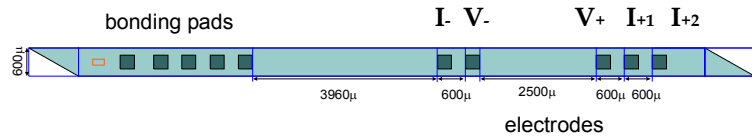


**Figure 3.9.** Five electrode probe. Its implementation is identical to that of MicroCard probe but for the experiment the electrodes were not platinized (see annex D).

As in the previous experiment, the results (Figure 3.10) showed that the five-electrode method reduced the error at low frequencies but was not capable to suppress it.

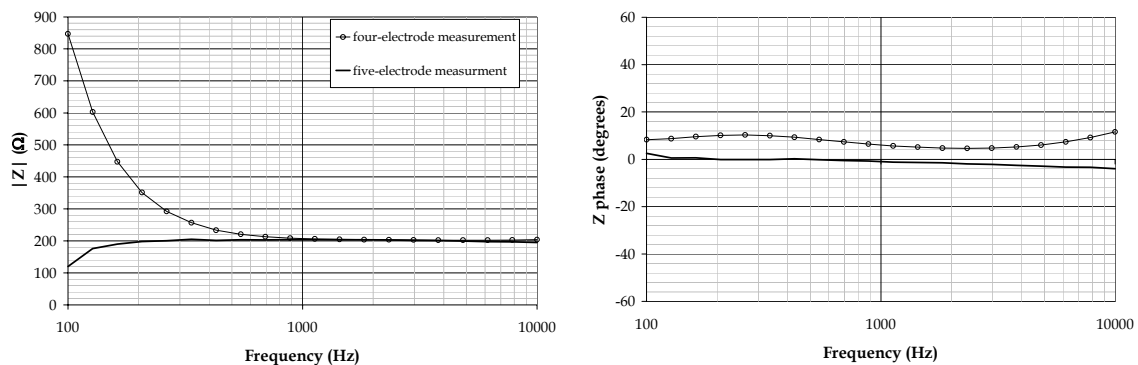


**Figure 3.10.** Results obtained with the five electrode silicon probe.

Then, the measurement set up was modified<sup>12</sup> to measure the electrode 4 impedance (current collector electrode, I) depending on the injection electrode ( $I_{+1}$  or  $I_{+2}$ ). Those impedances are not the same than those during both four-measurements but their differences should be in the same order of magnitude and that is enough to estimate the magnitude of the error.

<sup>12</sup> The  $V_{LO}$  terminal of SI 1260 was tied to the current input and the  $V_{HI}$  terminal was connected the V-electrode. In this way, although  $Z_{E4}$  is not exactly measured, the accuracy is enough for the purpose of the experiment.

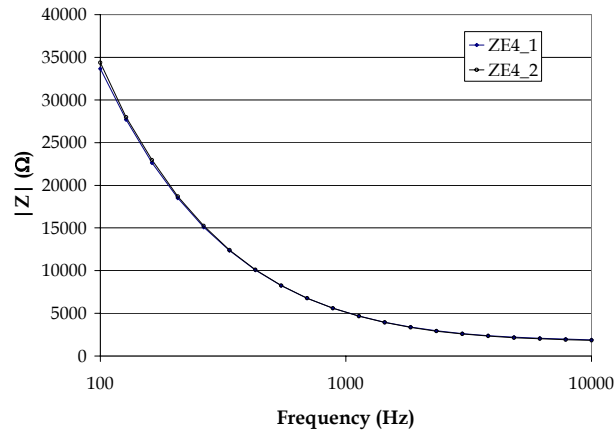


**Figure 3.11.** Impedance magnitude of electrode 4 (I) depending on the injection electrode ( $I_{+1}$  or  $I_{+2}$ ).

Although the difference between both measurements is small (Figure 3.11), the multiplicative factor for the error (equation 3.15) can have values up to 0.1 and that implies that the error at low frequencies will be significant. As it can be observed in Figure 3.12, the absolute values of the error estimated in this way are quite similar to the actual error values. Therefore, this experiment confirms that the electrode impedance modification could be the cause of the inability of the five-electrode method to suppress the errors at low frequencies

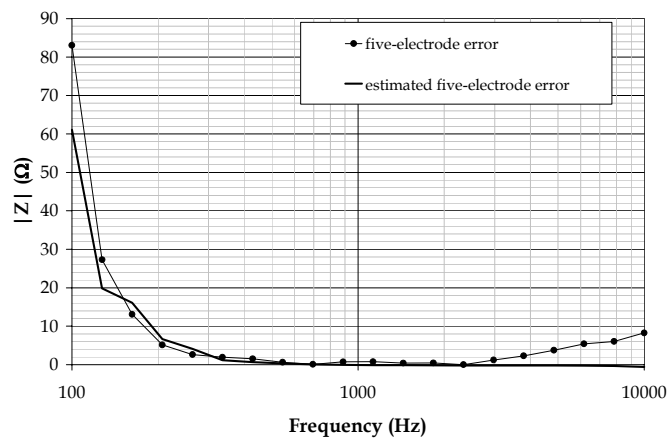


**Figure 3.12.** Actual five-electrode impedance magnitude error and its estimation according to the modification of electrode 4 (I) impedance.

It must be noted that in the above experiments the source of SI 1260 has been configured as a current source. That is, the same current was flowing through the electrodes in both measurements. Otherwise, in the case that the current is not controlled, since the electrode impedance is not linear, the electrode impedance

differences will be larger and the five-electrode error will be more severe. That has been experimentally verified.

In principle, by using equation 3.8, it could be possible to obtain error free five-electrode measurements if the impedance of electrode 4 is measured at the same time that the four-electrode measurements are performed. This was experimentally tried and, although it indeed improved the compensation, the overall performance was poorer since the set-up to measure  $Z_{E4}$  made worse the CMRR. Moreover, the complexity of the method was too high for practical purposes.

Another drawback of the five-electrode method it is found when analyzing the effect of random additive errors, such as noise, between both measurements:

$$Z_1 = Z_{m1} - \frac{Z_{E4}}{\text{CMRR}_T} \pm \varepsilon_1 \quad (3.16)$$

$$Z_2 = Z_{m2} - \frac{Z_{E4}}{\text{CMRR}_T} \pm \varepsilon_2 \quad (3.17)$$

$$Z_1 = Z_{C1} + \varepsilon = \frac{\lambda}{\lambda - 1} \cdot (Z_{m1} - Z_{m2}) + \varepsilon \quad (3.18)$$

↓

$$\varepsilon = \frac{\lambda}{\lambda - 1} \cdot (\pm \varepsilon_1 \pm \varepsilon_2) \quad (3.19)$$

That is, the effect of noise on the five-electrode method will be severe if  $\lambda$  value is not quite larger than the unity.

In conclusion, although the five-electrode method works and it could be useful in some applications such as those based on the measurement of low conductance homogeneous materials, its use is not advisable in the case of living tissues since the heterogeneity will cause larger  $Z_{E4}$  differences than those observed in the case of a saline solution and the overall performance will be similar to the four-electrode performance if not worse. As a consequence, the five-electrode method has not been used in the framework of this thesis work for living tissue impedance measurements.



## References

1. Sekiguchi, N., Komeda, T., Funakubo, H., Chabicovsky, R., Nicolics, J., and Stangl, G., "Microsensor for the measurement of water content in the human skin," *Sensors and Actuators B*, vol. 78 pp. 326-330, 2001.
2. Salter, D. C., "Examination of stratum corneum hydration state by electrical methods," *Curr Probl Dermatol Basel*, vol. 26 pp. 38-47, 1998.
3. Huysmans, M. C. D. N. J. M., Longbottom, C., Pitts, N. B., Los, P., and Bruce, P. G., "Impedance spectroscopy of teeth with and without approximal caries lesions- an vitro study," *J Dent Res*, vol. 75, no. 11, pp. 1871-1878, 1996.
4. Yamada, T., Hirose, H., Mori, Y., Onitsuka, A., Hayashi, M., Senga, S., Futamura, N., Sakamoto, K., Sago, T., Takagi, H., Yasumura, M., and Iwata, H., "Dielectric Spectrogram for Evaluating Ischemic Microstructural Changes of the Liver in Simple Cold Preservation," *Surgery Today*, vol. 32 pp. 1058-1063, 2002.
5. Geddes, L. A. Who introduced the tetrapolar method for measuring resistance and impedance? *IEEE Engineering in Medicine and Biology Magazine* 15[5], 133-134. 1996.  
Ref Type: Magazine Article
6. Pallás-Areny, R. and Webster, J. G., "AC instrumentation amplifier for bioimpedance measurements," *IEEE Transactions on Biomedical Engineering*, vol. 40, no. 8, pp. 830-833, Aug.1993.
7. McAdams, E. T., "Effect of surface topography on the electrode-electrolyte interface impedance, 1. The High Frequency ( $f > 1$  Hz), Small Signal, Interface Impedance - A Review," *Surface Topography*, vol. 2 pp. 107-122, 1989.
8. Bragos, R., Casas, O., Rosell, J., Riu, P. J., Rodriguez-Sinovas, A., and Cinca, J. Detection of healed myocardium scar in pigs measuring the electrical impedance spectrum with a percutaneous catheter. 63-66. 2001. Oslo, Norway. Proceedings of the XI International Conference on Electrical Bio-Impedance. 17-6-0001.  
Ref Type: Conference Proceeding
9. Kinouchi, Y., Iritani, T., Morimoto, T., and Ohyama, S., "Fast in vivo measurements of local tissue impedances using needle electrodes," *Med.Biol.Eng.Comput.*, vol. 35 pp. 486-492, 1997.
10. Bard, A. J. and Faulkner, L. R., *Electrochemical methods* New York: John Wiley & Sons, 1980.
11. Foster, K. R. and Schwan, H. P., "Dielectric properties of tissues and biological materials: a critical review," *CRC Critical Reviews in Biomedical Engineering*, vol. 17 pp. 25-104, 1989.
12. Weiss, T. F., "Voltage-gated ion channels," *Cellular biophysics - volume 2: electrical properties* Cambridge, Massachusetts, USA: The MIT Press, 2004, pp. 351-509.
13. Grimnes, S. and Martinsen, Ø. G., *Bioimpedance and bioelectricity basics* London: Academic Press, 2000.
14. Schwan, H. P., "Linear and nonlinear electrode polarization and biological materials," *Annals of Biomedical Engineering*, vol. 20 pp. 269-288, 1992.
15. Geddes, L. A., *Electrodes and the measurement of bioelectric events* New York: Wiley-Interscience, 1979.

16. McAdams, E. T. and Jossinet, J., "The detection of the onset of electrode-electrolyte interface impedance nonlinearity: a theoretical study," *IEEE Transactions on Biomedical Engineering*, vol. 41, no. 5, pp. 498-500, May 1994.
17. Chilbert, M. A., "High-voltage and high-current injuries," in Reilly, J. P. (ed.) *Electrical stimulation and electropathology* Cambridge, USA: Cambridge University Press, 1992, pp. 383-428.
18. Olson, W. H., "Electrical safety," in Webster, J. G. (ed.) *Medical instrumentation, application and design* Third edition ed. New York: John Wiley & Sons, 1998, pp. 623-658.
19. Steendijk, P., Mur, G., Van Der Velde, E. T., and Baan, J., "The Four-Electrode Resistivity Technique in Anisotropic Media: Theoretical Analysis and Application on Miocardial Tissue *in Vivo*," *IEEE Transactions on Biomedical Engineering*, vol. 40, no. 11, pp. 1138-1148, 1993.
20. Reilly, J. P., "Cardiac sensitivity to electrical stimulation," in Reilly, J. P. (ed.) *Electrical stimulation and electropathology* Cambridge, USA: Cambridge University Press, 1992, pp. 180-230.
21. Rosell, J. and Riu, P. J., "Common-mode feedback in electrical impedance tomography," *Clin.Phys.Physiol.Meas.*, vol. 13, Suppl. A, no. 4, pp. 11-14, 1992.
22. Nebuya, S., Noshiro, M., Brown, B. H., Smallwood, R. H., and Milnes, P., "Accuracy of an optically isolated tetra-polar impedance measurement system," *Med.Biol.Eng.Comput.*, vol. 40 pp. 647-649, 2002.



